© 2014. Published by The Company of Biologists Ltd | The Journal of Experimental Biology (2014) 217, 2358-2370 doi:10.1242/jeb.098426

RESEARCH ARTICLE

Level locomotion in wood ants: evidence for grounded running

Lars Reinhardt* and Reinhard Blickhan

ABSTRACT

In order to better understand the strategies of locomotion in small insects, we have studied continuous level locomotion of the wood ant species *Formica polyctena*. We determined the three-dimensional centre of mass kinematics during the gait cycle and recorded the ground reaction forces of single legs utilising a self-developed test site. Our findings show that the animals used the same gait dynamics across a wide speed range without dissolving the tripodal stride pattern. To achieve higher velocities, the ants proportionally increased stride length and stepping frequency. The centre of mass energetics indicated a bouncing gait, in which horizontal kinetic and gravitational potential energy fluctuated in close phase. We determined a high degree of compliance especially in the front legs, as the effective leg length was nearly halved during the contact phase. This leads to only small vertical oscillations of the body, which are important in maintaining ground contact. Bouncing gaits without aerial phases seem to be a common strategy in small runners and can be sufficiently described by the bipedal spring-loaded inverted pendulum model. Thus, with our results, we provide evidence that wood ants perform 'grounded running'.

KEY WORDS: *Formica polyctena*, Arthropod, Ground reaction force, Insect biomechanics, Ant locomotion, Grounded running

INTRODUCTION

Among insects, extremely fast and agile species exist that can easily adapt their locomotor performance to a variety of substrates and inclines (Graham and Cruse, 1981; Full and Tu, 1991; Duch and Pflüger, 1995; Larsen et al., 1995; Pelletier and Caissie, 2001; Goldman et al., 2006; Gladun and Gorb, 2007; Seidl and Wehner, 2008; Sponberg and Full, 2008; Weihmann and Blickhan, 2009). For example, experiments on the desert ant *Cataglyphis fortis* revealed running speeds of up to 50 body lengths per second on level ground (Seidl and Wehner, 2008; Weihmann and Blickhan, 2009). Similar relative velocities were also measured in the cockroach species *Periplaneta americana* (Full and Tu, 1991).

From a biomechanical point of view, questions regarding principles of locomotion or commonly used type of gait arise. It is well known that insects maintain the alternating tripodal gait pattern without aerial phases over wide ranges of speeds and slopes (Hughes, 1952; Delcomyn, 1971; Full et al., 1991; Full and Tu, 1991; Zollikofer, 1994; Goldman et al., 2006; Seidl and Wehner, 2008; Weihmann and Blickhan, 2009). Only at their highest speeds and in individual cases does *P. americana* change to quadrupedal and bipedal running (Full and Tu, 1991).

The faster locomotion of cockroaches was characterised as a bouncing gait, in which horizontal kinetic and gravitational potential energy of the centre of mass (CoM) change in phase (Full and Tu, 1990). This pattern of energy fluctuations is typical for running, trotting or hopping in various animals and can be described by simple spring-loaded inverted pendulum (SLIP) models (Blickhan and Full, 1993). In addition, SLIP-accordant ground reaction force patterns were determined in cockroaches. While the SLIP model is valid for the sagittal plane, an analogous model for the horizontal plane – the lateral leg-spring (LLS) model – has already been developed and validated with cockroaches (Schmitt et al., 2002). The SLIP model consists of a point mass on top of a compliant spring, which is compressed during the first half of stance and decompressed in the second half. Hence, the CoM reaches its minimum height during midstance and at the same time has the lowest speed. This is different from the situation in the inverted pendulum (IP) model, which is used as a standard model for a walking gait (Cavagna et al., 1976). In this model, through vaulting over a stiff supporting leg, a cyclic exchange from kinetic to potential energy and vice versa is achieved and the CoM describes a circular path with the highest point and the lowest velocity at midstance. In reality, stiff legs rarely occur and CoM dynamics is better described by a bipedal spring-loaded inverted pendulum (BSLIP) (Geyer et al., 2006) both for walking and for bouncing gaits with double support phases. This model has been adapted to experimental data of different gaits in humans, horses, quails and cockroaches (Geyer et al., 2006; Srinivasan and Ruina, 2006; Srinivasan and Holmes, 2008; Lipfert et al., 2012; Andrada et al., 2013b; Andrada et al., 2013a). Despite leg compliance, the lift of the CoM at midstance remains the criterion for a walking gait whereas lowering the CoM indicates a bouncing gait. In both gaits, inertia contributes to energy conversion and recovery. Mechanical energy can be stored and released as elastic energy through spring elements or kinetic and potential energy can be transformed into each other by a pendular exchange (Cavagna et al., 1964; Cavagna et al., 1976; Heglund et al., 1982).

To distinguish between bouncing and vaulting mechanics, two measures can be considered: (i) the percentage of energy recovery and (ii) the percentage of congruity (Cavagna et al., 1976; Ahn et al., 2004). Congruity conveys the similarity between the curve progressions of kinetic and potential energy (Ahn et al., 2004). Thus, a congruity of 100% is the result when the two curves have an identical trend throughout the whole gait cycle. Correspondingly, congruity amounts to 0% in the case of the IP and 100% in the SLIP model. The percentage of recovery expresses the magnitude of energy exchanged between potential and kinetic energy by the pendular mechanism (Cavagna et al., 1976). The two energy forms are out of phase in the IP and consequently the percentage of energy recovery approaches 100%. This value, however, cannot be reached because of losses in the collision (Ruina et al., 2005). While running, there is no exchange between these energies in the SLIP, and energy recovery amounts to 0% in this conservative model. Depending on the stiffness of the legs and style, the BSLIP model recovery can assume all values between 0% and 100% (ignoring collision loss). The recovery values measured for the cockroach

Science of Motion, Friedrich-Schiller-University Jena, Seidelstr. 20, 07749 Jena, Germany.

*Author for correspondence (lars.reinhardt@uni-jena.de)

Received 14 October 2013; Accepted 30 March 2014

The Journal of Experimental Biology

The Journal of Experimental Biology (2014) doi:10.1242/jeb.098426

List of symbols and abbreviations

a_x	acceleration in the x-direction
a_y	acceleration in the y-direction
a_z	acceleration in the z-direction
BSLIP	bipedal spring-loaded inverted pendulum
CoM	centre of mass
E_{kin}	kinetic energy
E_{pot}	potential energy
E_{tot}	total energy
f	stepping frequency
$\mathbf{F}_x$	force in the anterio-posterior direction
$\mathbf{F}_y$	force in the lateral direction
$\mathbf{F}_z$	force in the vertical direction
GRF	ground reaction force
h_{CoM}	CoM height
IP	inverted pendulum
LLS	lateral leg-spring
s_{co}	contact width
s_{cy}	stride length
SLIP	spring-loaded inverted pendulum
s_{sw}	swing width
t_{co}	contact time
t_{cy}	cycle time
t_{sw}	swing time
v	speed
v_x	velocity in the x-direction
v_y	velocity in the y-direction
v_z	velocity in the z-direction
x	anterio-posterior direction
y	lateral direction
z	vertical direction
α	thorax–substrate angle
β	caput–thorax angle
γ	caput–substrate angle
δ	gaster–thorax angle
ε	gaster–substrate angle
ζ	thorax–x-axis angle

varied with a mean of 15.7%, supporting a bouncing gait (Full and Tu, 1990).

Elastic structures in the legs are advantageous for bouncing gaits. As the joint axes are aligned vertically in the hindleg of cockroaches, the exoskeleton can operate as an energy-conserving spring during running (Dudek and Full, 2006). However, this does not apply for all insect species. For instance, in the case of ants, the leg plane is orientated perpendicular to the substrate. Consequently, the joint axes are orientated parallel to the ground and the exoskeleton cannot function as a passive spring element without the contribution of muscles and apodemes in the joints. Nevertheless, because of the existence of resilin, a certain degree of passive elasticity cannot be ruled out in the ant leg (Weis-Fogh, 1960). This long-chained protein is ideally suited as an energy store and has been found between the leg segments of several insects (Andersen, 1963; Andersen, 1964; Andersen and Weis-Fogh, 1964; Alexander, 1966; Anderson, 1966; Sannasi, 1969; Neff et al., 2000; Bennet-Clark, 2007; Patek et al., 2011; Michels and Gorb, 2012).

However, it is unclear to what extent resilin may support bouncing dynamics and, furthermore, the magnitude of energy recovery mechanisms in small insects has not yet been elucidated. It has even been argued that animals weighing less than 1 kg are not using energy recovery and locomotion is generated and maintained by muscle contraction alone (Reilly et al., 2007). In addition, the influence of relative friction and viscosity (damping ratio) of the limbs is notably higher in ants than in larger animals, as a result of their extremely low mass and size (Garcia et al., 2000). Moreover, forces like drag and those involved in securing a foothold also hinder propulsion (Full and Koehl, 1993; Federle et al., 2000), and the energetic cost of locomotion is disproportionately high (Full, 1991).

From this point of view, it is difficult to predict which movement strategy ants are using. The concepts on global CoM dynamics (IP and SLIP models) introduce virtual legs, which are generated by the co-operation of the legs constituting the tripod. Using compliant legs (BSLIP model), walking gaits are possible with much reduced vertical excursions of the CoM. Furthermore, the virtual leg may pivot about a virtual hip located above the animal. Nevertheless, considering the findings in other insects, we expected to find a bouncing gait, if inertia plays any role for an insect of such a small size. In order to examine this issue, we analysed the three-dimensional CoM kinematics of *Formica polyctena* Förster 1850, and measured its ground reaction forces (GRFs).

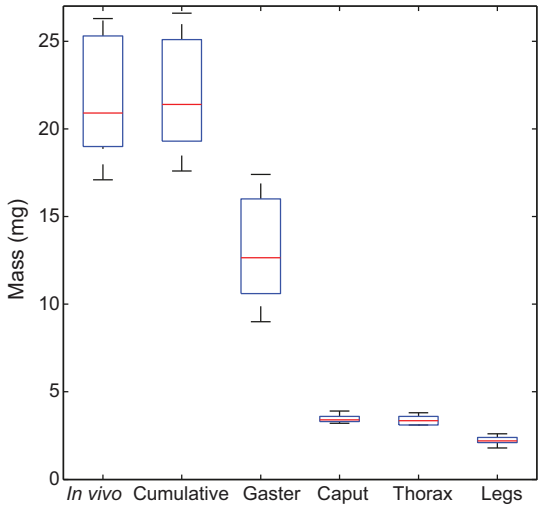

Fig. 1. Boxplot results of the segment mass distribution. The upper and lower parts of the blue box represent the interquartile range and the red line is the median. Black bars extending from the box indicate the highest and lowest values, excluding outliers.

RESULTS

Mass distribution

The results of the mass distribution are given in Table 1 and Fig. 1. The cumulated segment masses resulted in the same values as the mass of the living animals (paired t-test, P=0.01). A large proportion (58%) of the total mass was concentrated in the gaster (abdomen). Accordingly, the total CoM has to be near this body part. The variability in the gaster mass (s.d. of 3.1 mg or 14%) was high because of its variable filling level (Josens et al., 1998). This variability completely determined the variability of the total mass of

Table 1. Average segment mass

	Gaster	Caput	Thorax	Σ Legs	Cumulative	Total (*in vivo*)
Mass (mg)	13.00±3.08	3.47±0.23	3.38±0.26	2.21±0.22	22.06±3.12	21.77±3.32
Relative mass	0.58	0.16	0.16	0.10		

N=10, means ± s.d.

The Journal of Experimental Biology (2014) doi:10.1242/jeb.098426

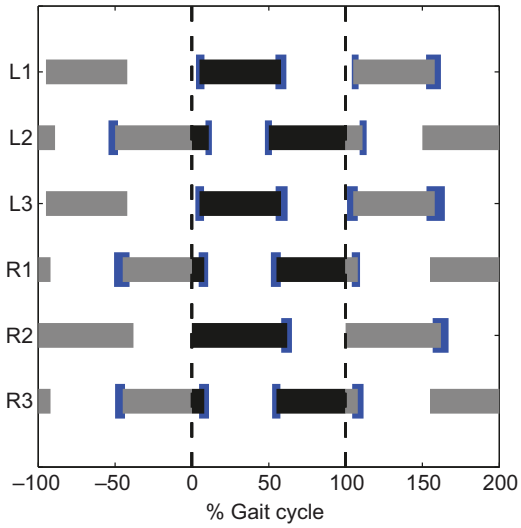

Fig. 2. Stride pattern of *Formica polyctena* at running speeds of 10.9±0.9 cm s^{-1}. Shown is the average temporal sequence of the ground contacts of all legs (left: L1–L3, right: R1–R3). The measures are normalised to the gait cycle time (black bars, 0–100%), which is defined by the right middle leg (R2). The extrapolated sequences of the previous (−100% to 0%) and subsequent (100% to 200%) steps are illustrated by grey bars. *N*=10. Means ± s.d. (s.d. indicated by blue areas).

the ant. Levene's test for homogeneity of variance revealed that the variances of the two groups do not differ (P=0.97). All other segments showed only minor variations of about 1% body mass. Moreover, the gaster mass strongly correlated with the total mass of the animals (Pearson correlation: r=0.98). The mass of all legs added up to only 10% of body mass and all had approximately the same size. Thus, the mass of a single leg does not exceed 2% of the ant's total mass.

Stride pattern

In our experiments, *F. polyctena* showed a tripodal stride pattern with no more than three legs in the air at any time. There were overlapping phases of both tripods (double support) in which all legs were on the ground partially. The middle leg initiated the contact phase and touched the ground a bit earlier than the other two legs of the same tripod (Fig. 2, R2). An average step cycle in the investigated velocity range (9.5–12.5 cm s^{-1}) lasted 85.8±3.2 ms (mean ± s.d.) which corresponds to a stepping frequency (f) of 11.7±0.4 Hz. For all legs, the contact phase was longer than the swing phase. This applied in particular to the middle legs, where the duty factor was 0.62 (see Table 2). At the front legs and hindlegs, the contact phase was clearly shorter and the duty factor accordingly smaller. Most step parameters were speed dependent (Fig. 3). With increasing speed (v), contact time (t_{co}) linearly decreased while swing time (t_{sw}) remained constant at about 35 ms (Fig. 3A). The intersection of the two regression lines was at 18.8 cm s^{-1}. Thus, at speeds above this value, the swing phase was longer than the ground contact and the duty factor fell below 50% (Fig. 3C). As expected, contact (s_{co}) and swing width (s_{sw}) increased with speed. Again, there was a linear relationship between the two variables and v (Fig. 3B). Stride length (s_{cy}) and stepping frequency (f) were also linearly dependent on speed (Fig. 3E,F).

Table 2. Selected stride parameters for velocities from 9.5 to 12.5 cm s^{-1}

	t_{co} (ms)	t_{sw} (ms)	t_{st} (ms)	Duty factor (t_{co}/t_{st})
Front leg	44.7±4.2	40.9±3.5	85.6±3.4	0.52±0.04
Middle leg	53.0±3.1	33.0±2.2	86.0±2.6	0.62±0.03
Hindleg	46.1±2.6	40.0±3.8	85.9±3.7	0.54±0.03

t_{co}, contact duration; t_{sw}, swing duration; t_{st}, stride duration.
N=10, means ± s.d.

Three-dimensional motion of the CoM

In a single step cycle, the CoM covered a distance of 9.4±0.7 mm in the anterio-posterior direction (Fig. 4, x). The forward speed of the CoM (v_x) rapidly decreased in the double support phase and steadily increased during the remainder of the gait cycle. Correspondingly, negative accelerations in the x-direction (a_x) were found during the double support. In the lateral direction (y), the CoM oscillated around zero. Around midstance the maximum lateral displacement of about 0.1 mm was reached at the side where two legs were on the ground, and subsequently the CoM swung back to the other side. On average the CoM was 2.5±0.4 mm above the ground (z) and fluctuated around this value sinusoidally with double step frequency. In the initial stance phase until the end of double support, the CoM was reduced by about 0.1 mm. Thereafter it was raised again to its highest point at midstance. In accordance with this, the vertical velocity was positive until midstance. In the phases where all legs were on the ground, accelerations of up to 5 m s^{-2} were registered.

CoM mechanics in the contact phase

For evaluating the gait dynamics, we calculated the CoM energetics during the contact phase of one tripod in all investigated steps. Besides linear regression analysis (Fig. 3G–I), the influence of running speed on CoM mechanics was determined by classifying the trials into two velocity groups using a median split. Thus, we obtained one sample with slower runs (group 1, v <11.5 cm s^{-1}, N=43) and one with faster runs (group 2, v >11.5 cm s^{-1}, N=42). In both group 1 and group 2, potential energy (E_{pot}) and kinetic energy (E_{kin}) proceeded nearly in phase in a sinusoidal pattern (Fig. 5A). A first minimum occurred in E_{pot} and E_{kin} at around 20–30% of contact. Kinetic energy reached its maximum value between 65% and 75% at all speeds. The maximum of the potential energy, i.e. the highest CoM position, was found between 60% and 80%, whereby the maximum was reached later at group 2. The CoM was raised at higher speeds (Fig. 5B, Table 3). Although the regression analysis revealed only a weak correlation (r^2=0.1) between v and h_{CoM} (Fig. 3G), we found significantly higher values for h_{CoM} (two-tailed t-test, P=0.02) in group 2. Consequently, the potential energy oscillated around a higher value in group 2 (0.56 µJ) compared with group 1 (0.48 µJ, see Fig. 5A). Because of the greater velocities (see Table 3), E_{kin} was higher in group 2 as well. For the percentage of mechanical energy recovery, we calculated values around 16–18% for the two speed ranges, which are not significantly different from each other (Fig. 5C, Table 3). In accordance with this, we found high values (60–70%, Fig. 5D, Table 3) for the congruity of the curve progressions of kinetic and potential energy. However, the comparison of means revealed significantly lower congruity values in group 2 than in group 1 (two-tailed t-test, P=0.02). Nevertheless, percentage congruity was on average higher than 50% in both groups, indicating a running gait.

Three-dimensional body kinematics

In Fig. 6 the trajectories of the body markers of all investigated steps as well as the tarsi positions of all legs are shown in the sagittal and horizontal plane in a body-fixed coordinate system. Tarsi positions are slightly curved (Fig. 6B). Consequently, during one contact

The Journal of Experimental Biology (2014) doi:10.1242/jeb.098426

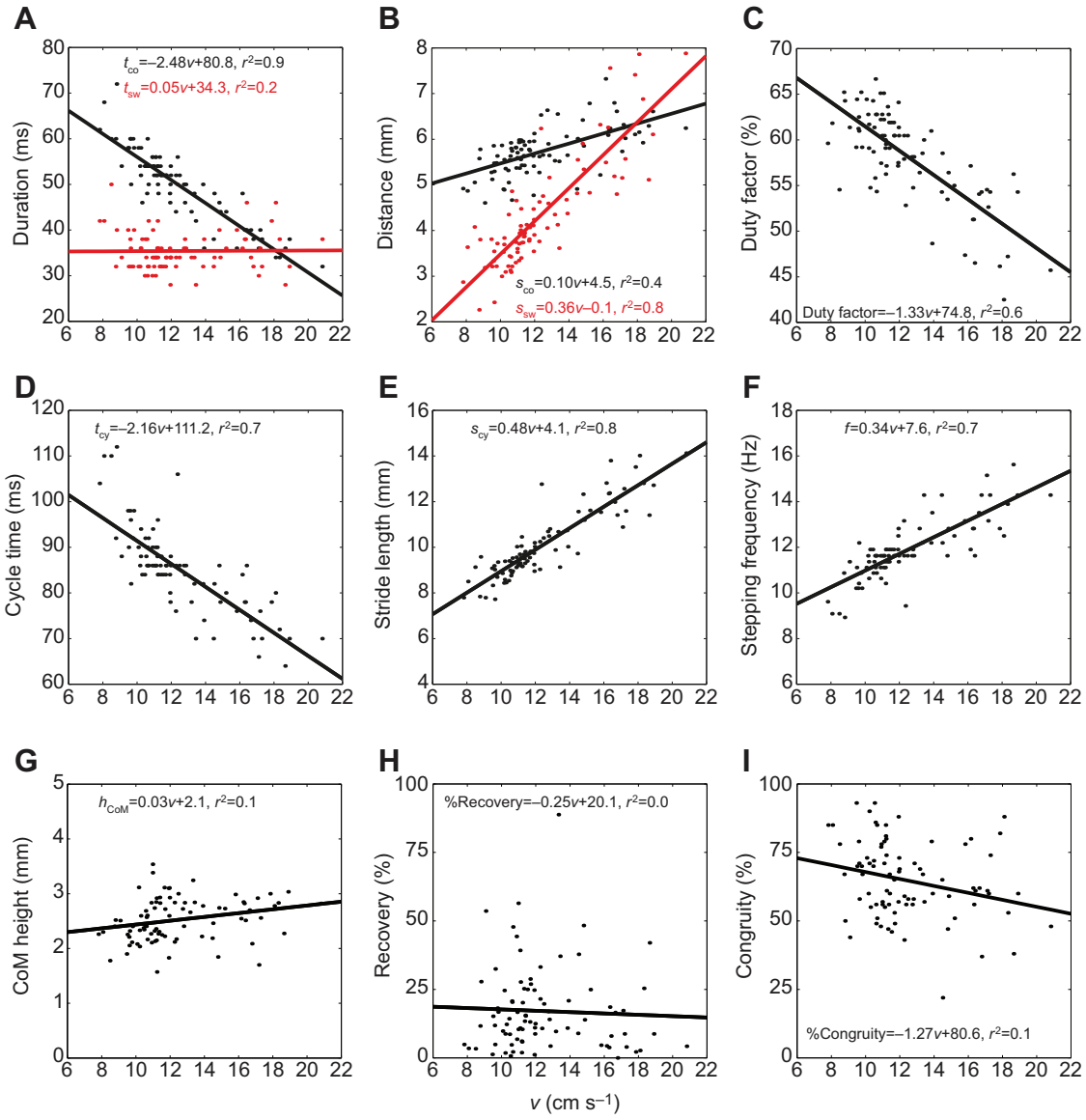

Fig. 3. Gait parameters relative to speed. Phase duration (A; t_{co}, contact time; t_{sw}, swing time), distance covered (B; s_{co}, contact width; s_{sw}, swing width), duty factor (C), cycle time (t_{cy}; D), stride length (s_{cy}; E), stepping frequency (f; F), mean centre of mass (CoM) height (h_{CoM}; G), percentage recovery (H) and percentage congruity (I) versus running speed (v). In A and B, black dots symbolise the values of the contact phase and red dots represent the swing phase (N=85). Linear regressions are designated by solid lines, and the equations are presented for each plot.

phase the CoM swung to the side where two legs were on the ground and back into the initial y-position. Marker B3 was located on average less than 0.3 mm away from the CoM. The points digitised more cranially (B1/B2) seemed to move along an arcuate path around a pivot point located close to the CoM (Fig. 6A). However, the gaster tip (B4) remained nearly at the same spot and kept its orientation (see below). Moreover, during the entire individual step cycle, the angular position of the three main segments to each other varied little. The peak-to-peak amplitudes of all rotational movements amounted to less than 5 deg (Fig. 7A). In particular, the angle between the caput and thorax (β) almost did not change, remaining at 139.4±1.9 deg (Table 4). The same applied to the gaster–substrate angle (ε), which on average remained at 41.4±2.3 deg with an angular velocity around zero (Fig. 7B). The most distinct rotational motion was the pitch movement of the thorax–caput complex around the petiolus and is reflected in α and δ. Because of the steady gaster position, they showed an almost identical cosinusoidal time course with two oscillations per gait cycle. On average, α oscillated around 22.7±2.3 deg while δ amounted to 161.3±2.3 deg. This rotation was performed at angular velocities of up to ±500 deg s^{-1} (Fig. 7B). We calculated the rotational energy of pitch and found maximum values of 0.4 nJ. These are about 50 times smaller than the fluctuations of the kinetic and potential energy of the CoM (Fig. 7C). On average, these two energy forms oscillated in a range of ±20 nJ with the same amplitudes. The yaw (ζ) angle had a sinusoidal profile around 0 deg with one oscillation per stepping cycle.

Three-dimensional GRFs

The front and middle leg pair generated only minor propulsive forces over the entire contact phase ($\mathbf{F}_x$>0, Fig. 8), and braked especially during the first half of stance. In contrast, the hindlegs produced relatively high positive forces in the running direction before slightly braking towards the end. In the lateral ($\mathbf{F}_y$) direction,

The Journal of Experimental Biology (2014) doi:10.1242/jeb.098426

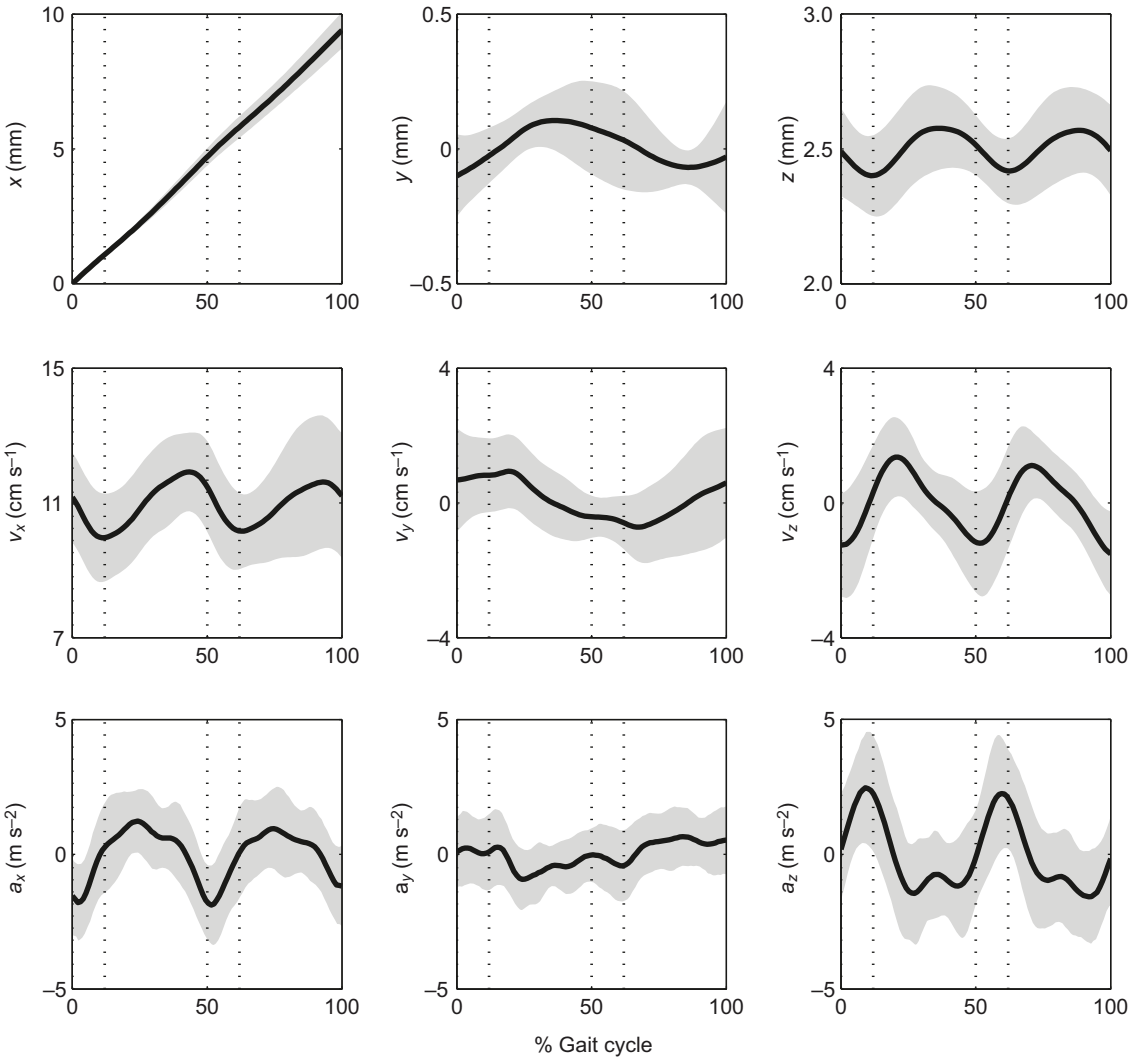

Fig. 4. Three-dimensional CoM kinematics in *F. polyctena*. Mean trajectories of CoM position, velocity and acceleration (*a*) during one gait cycle are shown in the coordinate system defined in Fig. 11C. The areas between the dashed vertical lines (0–12% and 50–62%) indicate phases when legs of both tripods were on the ground. Mean values are shown as solid black lines and s.d. as grey areas. The investigated animals weighed 20.2±3.0 mg and ran with an average speed of 10.9±0.9 cm s^{-1}. Presented curves were calculated from all measurements of animals in the velocity range from 9.5 to 12.5 cm s^{-1} (*N*=50).

the middle leg as well as the hindleg produced consistently negative forces (i.e. pressing them outward). However, we registered no significant forces in the lateral direction in the front legs. All legs generated positive, substrate-normal forces (pressing on the substrate), whereby the time courses of the middle leg and hindleg were very similar. Up until 30% of stance, both time courses steeply increased up to 0.5 body weight and subsequently fell off continuously. At midstance, the three legs all had the same force values (one-third body weight). The front legs generated the same vertical force over a major part of the contact. Thus, the body weight was shifted more and more towards the cranial legs. With knowledge of the individual leg forces and the stride pattern, we calculated the total leg-generated force acting on the CoM (Fig. 9A). While the vertical ($\mathbf{F}_z$, red) and fore-aft force ($\mathbf{F}_x$, blue) went through two cycles per step, only one period was seen in the lateral direction ($\mathbf{F}_y$, green). $\mathbf{F}_z$ on average corresponded to body weight and oscillated around this value with an amplitude of 0.4 body weight. After the overlap phase until midstance, this force was higher than the weight force. The maximum force was generated at about 20% and 70% of the gait cycle and then continuously decreased until the next double support to its minimum. $\mathbf{F}_x$ oscillated around zero and was negative during double support. At around midstance, this force component reached its maximum of 0.3. $\mathbf{F}_y$ fluctuated around zero in a sinusoidal pattern with amplitudes below 0.1.

Subsumption

In the following paragraph, we use a representative image sequence (Fig. 10) to describe the stepping pattern, the kinematics and dynamic contributions of the individual legs during level locomotion in *F. polyctena*. This comprehensive description provides the background for the considerations in the Discussion. All three legs can be considered as two-segmented in a simplified manner. Viewed in the sagittal plane, the distal segment (tibia, metatarsus and tarsus) of the front leg reaches the ground at an angle of about 50 deg at the moment of touchdown, while the femur is orientated ~10 deg to the horizontal. Consequently, the angle between the two segments is around 120 deg. In the course of stance, this angle decreases up to 55 deg while the distal segment tilts over the contact point and the angle of attack is around 110 deg at lift-off. Meanwhile, the hindleg extends during the stance phase. As a result, the angle in the

The Journal of Experimental Biology (2014) doi:10.1242/jeb.098426

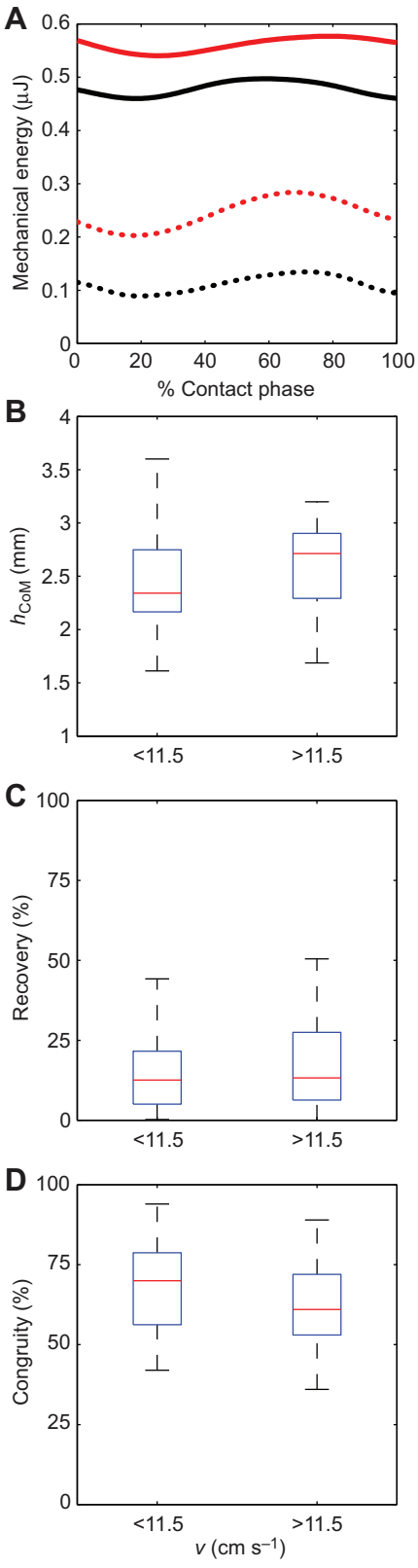

Fig. 5. CoM energetics of the contact phase at different speed ranges. The investigated trials (N=85) were divided into two velocity groups, ranging from 7.8 to 11.5 cm s^{-1} (N=43, black), and from 11.5 to 20.8 cm s^{-1} (N=42, red). (A) The mean trajectories of the potential (solid lines) and kinetic (dotted lines) energy. (B–D) The boxplots compare the average h_{CoM}, the percentage recovery of mechanical energy (see Cavagna et al., 1976) and the percentage congruity (see Ahn et al., 2004) between the two groups.

femur–tibia joint increases from around 55 to 140 deg while the approach angle of the distal segment decreases from 65 to 30 deg. A different situation exists in the middle leg, as it operates sideways in an extended position. The almost constant angle in the femur–tibia joint causes only small changes in the effective leg length, i.e. the distance between coxa and tarsus tip. Because the coxa height is the same, these changes can be determined in the top view and amount to less than 7%. The angle of attack of the effective leg ranges between 25 and 30 deg. This happens while the leg is loaded with a large portion of the body weight, especially in the vertical and lateral direction and particularly during the first half of stance ($\mathbf{F}_y$ and $\mathbf{F}_z$, Fig. 8). Thus, a relatively high leg stiffness is indicated, which is sufficient to compensate for the lateral forces of the contralateral legs. This would cause the CoM to be slightly deflected to the side if two legs were on the ground (y, Fig. 4 and Fig. 6B). However, when considering the sagittal projection, the leg is clearly compressed during midstance. Compared with the length at the moment of touchdown or lift-off (2.8 mm), effective leg length is reduced by 18% at midstance. An even greater shortening can be found in the front leg. The sagittal coxa–tarsus distance decreases from about 4.5 mm at touchdown to 3 mm at midstance and finally to 2.5 mm at lift-off. Thus, leg length is reduced by 33% in the first half of the contact phase, and by another 11% in the second half. This happens mainly through flexion in the femur–tibia joint, which causes erection of the femur and forward pitching of the thorax (decreasing α, Fig. 7A). The gaster position (i.e. its height and its angle to the substrate, ε, Fig. 7A), remains unaffected by pitch. Instead, its fluctuations are erratic, uncoordinated and clearly decoupled from the thorax oscillations (Fig. 7B). In this process, the front leg is braking ($\mathbf{F}_x$<0, Fig. 8) before it contributes slightly to propulsion in the second part of contact ($\mathbf{F}_x$>0, Fig. 8). As the hindleg is pushing forward as well, running speed (v_x, Fig. 4) and kinetic energy (E_{kin}, Fig. 5A and Fig. 7C) continue to increase until the legs of the other tripod hit the ground.

DISCUSSION

Tripod conservation

Similar to other fast-moving insects, the walking legs of wood ants are organised in stereotyped alternating tripods. The front and rear leg of one side and the middle leg of the other side move simultaneously during a step, while each moves out of phase with its contralateral pair (Hughes, 1952; Delcomyn, 1971; Zollikofer, 1994). Throughout the entire contact period a statically stable situation was ensured, as the CoM (Fig. 10, red dot) was always within the support area of the tripod (Ting et al., 1994).

In our experiments, we found no significant adaptions in gait dynamics to running speed over the investigated range from 7.8 to 20.8 cm s^{-1} (10–26 body lengths s^{-1}). In none of the recorded video sequences was a flight phase observed and the tripodal gait pattern with double support phases was instead maintained. As shown in Fig. 3C, the duty factor decreased linearly with increasing speed. At speeds of 8 cm s^{-1}, this parameter was around 0.65. Through linear regression, we estimated that the duty factor should fall below 0.5 at a velocity of ~19 cm s^{-1}. Consequently, the double support phase should disappear and flight phases occur. Thus, taking the flight phase as a criterion, a gait change would be the result. However, this could not be proven, although we determined values below 0.5 in a few trials. This is most likely to be due to measurement inaccuracies. As the sample rate of kinematics was 500 Hz, phase durations could only be determined with an error of ±4 ms. Based on linear regression analysis we expect a gait cycle time of around 70 ms at running speeds near 20 cm s^{-1} (Fig. 3A). With an assumed

The Journal of Experimental Biology (2014) doi:10.1242/jeb.098426

Table 3. Average centre of mass energetics of the contact phase at two speed ranges

Group	Speed range (cm s^{-1})	*N*	Mean speed (cm s^{-1})	h_{CoM} (mm)	Recovery (%)	Congruity (%)
1	<11.5	43	10.31±0.14	2.43±0.39	16.15±14.70	68.98±13.87
2	>11.5	42	14.61±0.39	2.62±0.38	18.12±16.75	61.48±14.13

h_{CoM}, centre of mass height.
Means ± s.d.

contact duration of 35 ms (duty factor of 0.5), the estimated duty factor can range between 0.42 and 0.59 within the specified range of error. As we could not find runs above 21 cm s^{-1} and we did not observe aerial phases, we conclude that *F. polyctena* does not perform a gait change. Therefore, we conclude that this is the maximum possible velocity of this species.

This assumption is confirmed by other studies on the closely related species *Formica pratensis*. In more than a hundred trials, the authors did not find velocities above 21.8 cm s^{-1} (Seidl and Wehner, 2008; Weihmann and Blickhan, 2009). The preferred speed range of *F. pratensis* was between 11 and 14 cm s^{-1}. Furthermore, a mean h_{CoM} of 1.9 mm with typical vertical oscillations of 0.1–0.2 mm was determined (Weihmann and Blickhan, 2009), which is congruent with our results. In addition, Seidl and Wehner found a linear relationship between speed and step frequency, with maximum values of 20 Hz in their fastest trials (Seidl and Wehner, 2008). In our fastest runs, the durations of the contact and swing phase were measured around 30 ms (Table 2 and Fig. 3A). This is associated with a stepping frequency of ~16 Hz (Fig. 3F). Across the investigated speed range, the swing phase duration remained nearly constant at 35.4±4.4 ms. Hence, we conclude that the ants always performed the swing phase as quickly as possible, probably in order to quickly reach ground contact again. As the step length is limited by leg length, higher velocities could only be achieved by higher step frequencies. This in turn means that both the contact and the swing time must be reduced if the duty factor should stay above 0.5. Thus, the maximum speed seems to be determined by the duration of the swing phase or rather the ability of the animals to perform this movement.

Vaulting or bouncing

At first glance, the absence of aerial phases and the related duty factors above 0.5 suggest a walking gait. This type of gait is typically described by the inverted pendulum model, whereby the CoM is vaulting over a stiff supporting leg (Cavagna et al., 1976). Following this model, it is to be expected that the CoM reaches its highest point at midstance. Furthermore, kinetic and potential energy should be out of phase, which would also be expressed in a high percentage of energy recovery and a small percentage of congruity (Cavagna et al., 1976; Ahn et al., 2004). Our findings do not support major energy exchange, as kinetic and potential energy are in phase for long periods of the contact phase (Fig. 5A and Fig. 7C). Accordingly, the congruity between the curve progressions of the two energy forms is relatively high. We determined congruity values of 60–70% and a recovery of 16–18% (Fig. 3H,I, Fig. 5C,D and Table 3). Furthermore, the CoM did not reach its highest point before 60% of stance time (Fig. 4 and Fig. 5A). These results appear to be consistent with those of the cockroach *Blaberus discoidalis*. Over a speed range from 0.08 to 0.66 m s^{-1} (2–16 body lengths s^{-1}), these fast-moving insects use the alternating tripod gait without aerial phases as well (Full and Tu, 1990). Furthermore, the maximum stride frequency of 13 Hz was very close to that of *F. polyctena*. For the cockroaches, recovery values varied around a mean of 15.7% and did not vary as a function of speed. This is equivalent to our calculations and led the authors (Full and Tu, 1990) to also reject the inverted pendulum model.

It should be noted that in the transition region between walking and bouncing (i.e. especially within the transition region to grounded running), the measures of recovery and congruity are ill-defined. This transition region is characterised by small excursions of the CoM. With diminishing vertical excursions of the CoM and constant variance, recovery approaches zero and the phase of the potential energy cannot be determined reliably. In our case, the vertical displacement of the CoM of about 10% body height is within the magnitude of the standard deviation.

However, even without aerial phases, the gait of cockroaches was classified as a bouncing gait (Full and Tu, 1990; Full et al., 1991; Blickhan and Full, 1993; Srinivasan and Holmes, 2008). This is not an isolated case as several species, such as birds, crabs, primates, horses, marsupials and elephants, show bouncing mechanics with duty factors above 0.5 (e.g. Alexander and Jayes, 1978; Blickhan and Full, 1987; Gatesy and Biewener, 1991; Kimura, 1996; Muir et al., 1996; Gatesy, 1999; Schmitt, 1999; Hutchinson et al., 2003; Schmitt, 2003; Srinivasan and Holmes, 2008; Biknevicius et al., 2013). These gaits are known by terms such as ‘compliant walking’ (Alexander and Jayes, 1978), ‘grounded running’ (Rubenson et al., 2004) or ‘Groucho running’ (McMahon et al., 1987). So far, the most suitable model to describe all these types of locomotion is the bipedal spring-mass

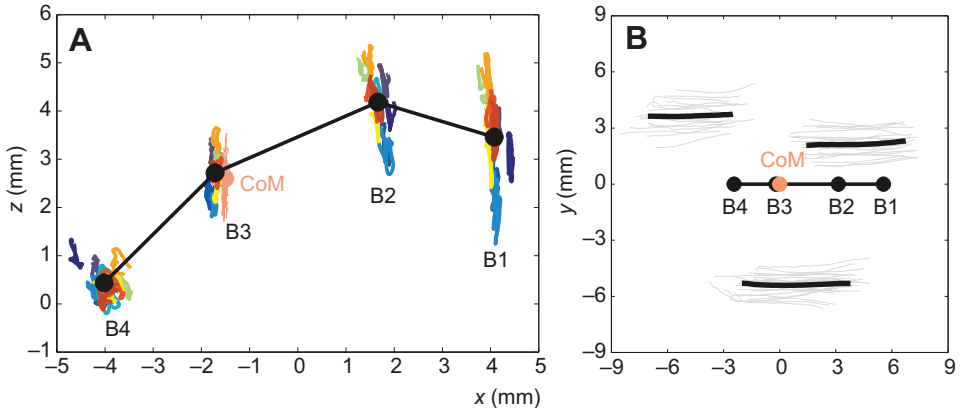

Fig. 6. Visualisation of the body movement during the gait cycle. (A) Trajectories of the digitised body markers (B1–B4) from 20 gait cycles of 10 runs in the sagittal plane. Each run was performed by a different individual ant and is shown in a different colour. Black lines and dots represent the mean body posture of all steps. The calculated position of the CoM is marked by a pink dot. (B) Position of the tarsi and body markers in the horizontal plane with respect to the CoM (pink dot). The trajectories of the individual experiments are shown as thin grey lines and the mean curves as thick black ones. The animal moves from left to right and the leg tips from right to left.

The Journal of Experimental Biology (2014) doi:10.1242/jeb.098426

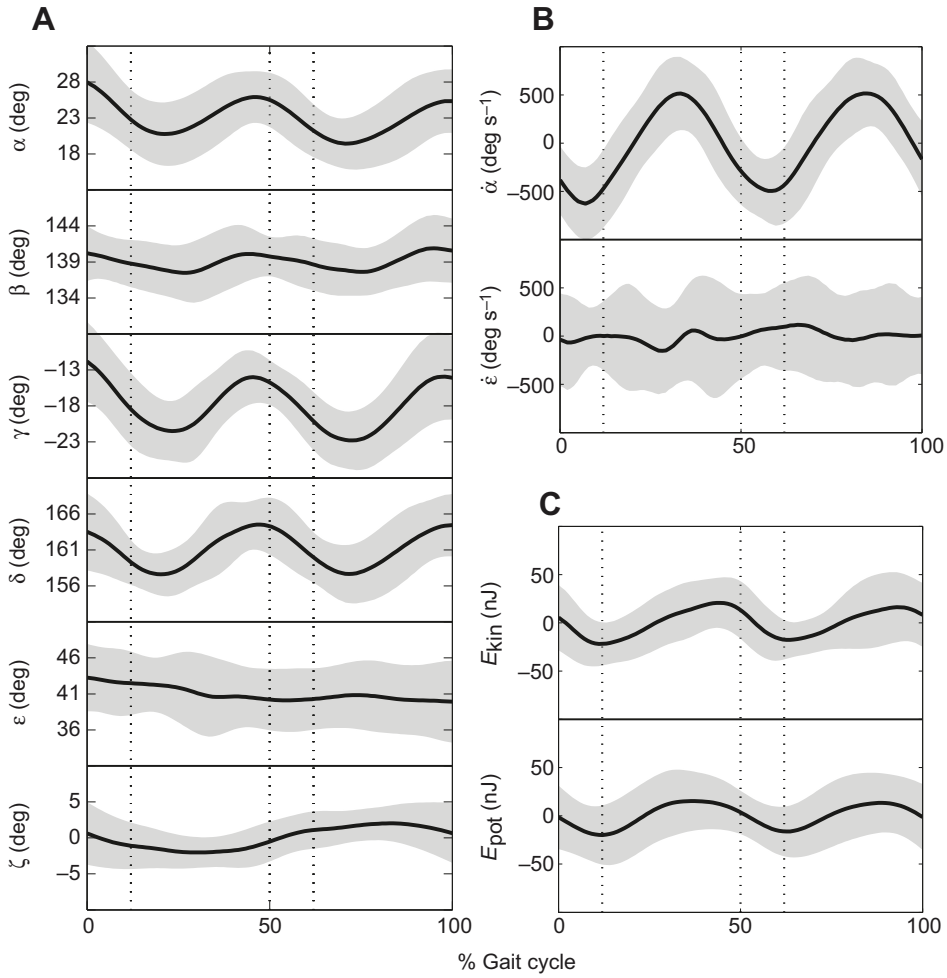

Fig. 7. Segment angles and CoM energetics. (A) Mean body angle trajectories during one gait cycle (*N*=20). α, thorax–substrate angle; β, caput–thorax angle; γ, caput–substrate angle; δ, gaster–thorax angle; ε, gaster–substrate angle; ζ, yaw (thorax–*x*-axis) angle. Note the different scales. (B) Angular velocities of two selected angles. (C) Fluctuations of CoM kinetic energy (in the *xy*-plane) and potential energy. Presented curves were calculated from all measurements of animals in the velocity range from 9.5 to 12.5 cm s^{-1}. Mean values are shown as solid black lines and s.d. as grey areas. The areas between the dashed vertical lines (0–12% and 50–62%) indicate phases when legs of both tripods were on the ground.

model (BSLIP) (Geyer et al., 2006). In this model, during compliant walking, the CoM is at its apex at midstance, similar to the inverted pendulum. Nevertheless, the BSLIP is purely conservative and entails energy storage. Correspondingly, energy recovery in the model is diminished to values less than 50%. Small birds, for example, only reached values around 30% during walking (Nyakatura et al., 2012). The BSLIP model can also be used to describe grounded running (Andrada et al., 2013a). In this gait, the CoM is not raised above its height at touch down, but double support is maintained. This gait seems to play a very prominent role in small animals with compliant legs (i.e. small birds). In these animals the recovery values during grounded running are about 7% (Nyakatura et al., 2012). Our findings give rise to the assumption that wood ants also use this type of locomotion. More specifically, the mechanical compliance, demonstrated in the front and middle leg of *F. polyctena*, leads to only small vertical oscillations of the CoM and supports nevertheless the maintenance of ground contact. We conclude that this is therefore very probably a main objective during locomotion in these animals.

Elastic elements in the insect leg

On the assumption that the investigated ants conducted grounded running, we hypothesise that elastic elements could be of advantage. As previously mentioned, a rubber-like protein called resilin is known as a component of the insect cuticle and can provide elasticity to the legs (Weis-Fogh, 1960). In cockroaches, resilin was studied at the tibio-tarsal joint and the articulation between the fourth and fifth tarsal segments of the hindleg (Neff et al., 2000). This spring-like elasticity in the cockroaches' hindleg was provided by resilin in connection with the exoskeleton (Dudek and Full, 2006). According to these authors, as much as 75% of the mechanical energy of the CoM may be returned each step. Moreover, 40% of the external mechanical work done to the CoM can be stored and returned because of the elasticity of the leg. Nevertheless, this is considered an overestimate of energy storage and return in this system and it is assumed that in reality these springs only contribute marginally in improving energetic efficiency in cockroaches (Patek et al., 2011). It is more likely that the leg springs function as a kind of shock absorber, which responds to perturbations more quickly than a neural signal could (Koditschek et al., 2004; Dudek and Full, 2006; Dudek and Full, 2007). Thus, locomotion can be stabilised by elastic legs. As resilin pads can be found within the joint apparatus, they are predestined to act as elastic antagonists to the leg muscles (Neff et al., 2000). In this way, it is possible to produce restoring forces without muscle activity. Additionally, it is also conceivable that this

Table 4. Mean body angles in the sagittal plane

α	β	γ	δ	ε
22.7±2.3 deg	139.4±1.9 deg	−17.9±2.7 deg	161.3±2.3 deg	41.4±2.3 deg

Means ± s.d.

The Journal of Experimental Biology (2014) doi:10.1242/jeb.098426

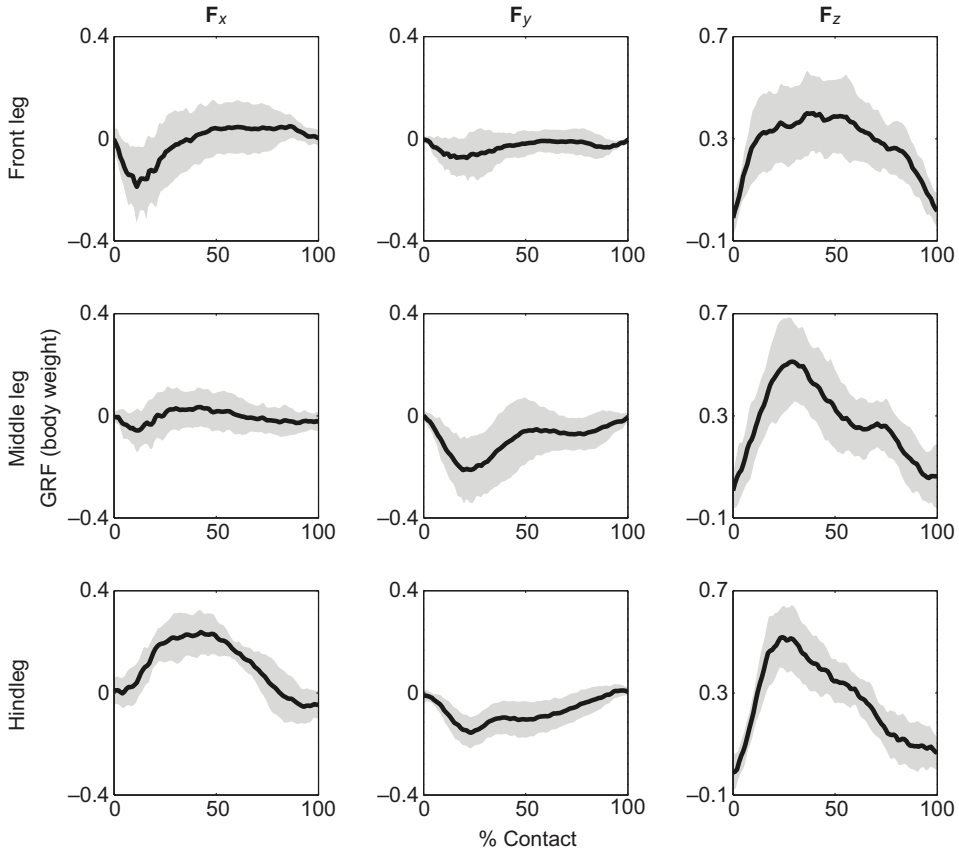

Fig. 8. Components of the ground reaction force of the legs. Curves are shown in the coordinate system defined in Fig. 11C. Mean values are shown as solid black lines and s.d. as grey areas. The ground reaction forces (GRFs) are normalised to body weight. A value of one corresponds to the weight force of the animal. The investigated animals weighed 20.9±3.9 mg and ran at a speed of 13.5±3.6 cm s^{-1}.

effect is used as a drive for the leg extension in the swing phase. As previously mentioned, leg compliance in the front leg of *F. polyctena* is mainly reached by flexion in the femur–tibia joint. This leads to an eccentric load of the leg extensor muscles during the contact phase. Therefore, we assume that there is a considerable contribution to leg compliance by muscle activity. However, in future studies, skeletal anatomy and muscle architecture of walking legs of fast running ant species should be examined in more detail to allow for a discrimination of the mechanisms.

Mechanical cost of transport

The investigated ants moved with a preferred speed of around 11 cm s^{-1}, a step length of ~9 mm and a step frequency of 12 Hz. Consequently, they pass 111 gait cycles in 9 s to cover a distance of 1 m. On their daily foraging trips, wood ants travel distances of up to 200 m (Kirchner, 2001). This amounts to 22,200 steps on level surfaces. However, the habitat of wood ants is far from flat and they permanently have to face obstacles along their path when moving over sticks and stones. Consequently, it can be assumed that they take many more steps to cover such distances in the wild. Furthermore, the locomotion is acyclic and intermittent, and therefore conditions for energy-saving mechanisms through pendular or spring mechanics are rather disadvantageous.

It has been unclear whether these strategies play a role in small animals, with a body mass below 1 kg (Reilly et al., 2007). Although the relative amount of external mechanical energy used to move the CoM is independent of body size, the metabolic costs of transport are much higher in smaller animals (Full, 1991; Reilly et al., 2007). Reilly et al. came to the conclusion that locomotion is generated and maintained by muscle contraction alone and that these animals benefit little from passive energy-saving mechanisms (Reilly et al., 2007). For lizards (mass 21 g) and squirrels (mass 238 g), they calculated that the metabolic energy saved by pendular exchange and elastic energy recovery is less than 2%. This holds especially true for the crouched posture, which is typical for small animals, and is associated with more abducted and flexed limbs and causes higher metabolic cost as a result of a higher muscular effort (Biewener, 1990; Reilly et al., 2007; Biknevicius et al., 2013). Furthermore, it was shown that metabolic costs are mainly reduced by an adjustment of the stepping frequency (Reilly et al., 2007). Experiments on stick insects, cockroaches and mice showed that passive forces of leg muscles and joint structures are relatively large in animals with low-weight limbs compared with gravitational forces (Garcia et al., 2000; Hooper et al., 2009). This is particularly reflected in a higher muscular activity during the swing phase in order to overcome these forces and results in a further increase of metabolic cost. Under these circumstances, running (i.e. bouncing dynamics) is preferred over walking in small animals (Garcia et al., 2000). The same probably also applies to ants and confirms the hypothesis that ants perform grounded running.

As the mass of the abdomen, which amounts to nearly 60% of the body mass (Table 1 and Fig. 1), swings independently from the rest of the body, these fluctuations do not contribute to the rhythmic changes of the body's rotational energy. The decoupling indicates a compliant connection and significantly reduces the amount of rotational energy of the animal's body.

GRFs

Because of the modified experimental procedure (see Materials and methods), we caused a behaviour modification in comparison to our previous studies (Reinhardt et al., 2009). In this way, exploratory behaviour was strongly reduced and the ants were trained on steady fast locomotion. Naturally, these changes were associated with changes in the GRFs. This is particularly evident in the substrate-

The Journal of Experimental Biology (2014) doi:10.1242/jeb.098426

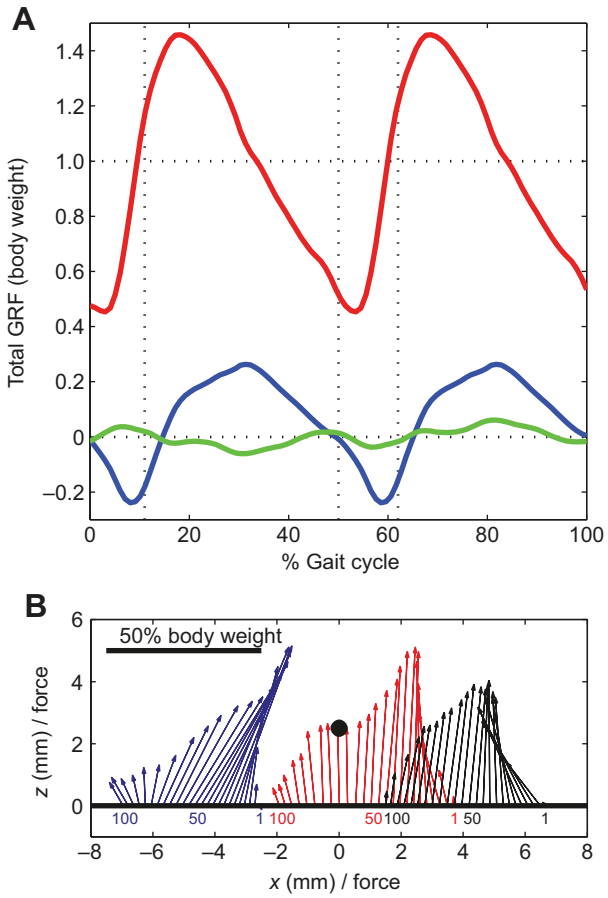

Fig. 9. Total force and force vectors. (A) Components of leg-generated force acting on the CoM, calculated as the sum of the single leg forces (mean curves in Fig. 8) during the gait cycle, taking into consideration the two phases of stance overlap (dashed grey lines). All values are normalised to body weight and gait cycle time. The fore–aft force ($\mathbf{F}_x$, blue) and lateral force ($\mathbf{F}_y$, green) oscillated around zero and the vertical force ($\mathbf{F}_z$, red) was positive throughout stance and fluctuated around the body weight with a net momentum of one. (B) Projection of the force vectors of the three legs in the sagittal plane during one stance phase: front leg (black), middle leg (red), hindleg (blue); black dot, CoM (0, 2.5). The animal moved from left to right and the leg tips (bases of the vectors at the *x*-axis in the *xy*-plane) moved from right to left with respect to the CoM. Coloured numbers at the bases define the following time points: beginning (1), midstance (50) and end of the contact phase (100).

parallel forces ($\mathbf{F}_x$, $\mathbf{F}_y$) of the front and middle leg. In the previous experiments, the lateral force of these legs showed a sinusoidal curve progression, which is equivalent to an initial outward pushing and a later inward pulling during the second part of stance. The situation was similar in the fore–aft force of the front leg, which firstly braked and later accelerated the body forwards. Our recent investigations determined a clearly smaller forward impulse of the front leg in the second part of the contact phase and no sign change in the lateral force of the middle leg. The front leg produced nearly no force in this direction. However, the middle leg hardly contributes to propulsion. Almost identical curve progressions were identified for the hindleg, again providing evidence for its role as the primary propulsion unit.

The force patterns of the first test series revealed similarities to vertically climbing cockroaches, which were particularly apparent in the lateral force component of the two front legs (Goldman et al., 2006; Reinhardt et al., 2009). The ants probably ensured ground contact through permanently clinging to the substrate by laterally pulling towards the midline during the second half of stance. Thus, the behaviour of the animals was primarily aimed at exploring the unfamiliar surroundings and not at overcoming a known path as fast as possible. This is also confirmed by the detected ground contact of the gaster tip, which is necessary to set up a pheromone trace (Horstmann, 1976). As the gaster touched the ground in none of the analysed trials of the current test series, we conclude that an ant trail was already established through the modified experimental procedure. As our results indicated, the ants ran significantly faster on this familiar path. Hence, it is assumed that the recent results, unlike the previous ones, reflect the fast, straight locomotion in *F. polyctena*.

When evaluating the GRFs more similarities emerge to those of fast running than to climbing cockroaches (see Full et al., 1991; Goldman et al., 2006). The vertical force component regularly predominates and the sagittal force vectors are therefore standing steep over a wide duration of the contact phase in all legs (Fig. 9B). Furthermore, no inward directed lateral forces were found in any leg. The sum of the leg-generated forces (Fig. 9A), which could be considered to be the total force acting on the CoM, oscillated in a similar manner (Full and Tu, 1990). In the fore–aft direction, an initial negative impulse is cancelled out by a positive one in the second half of stance. The amplitude was around 0.2 body weight and thus similar to that of *F. polyctena*. Similar to our experiments, the vertical component fluctuated bimodally around the body weight, whereby the maximum value was not larger than 1.5. Following the calculations of Andrada et al. (Andrada et al., 2013a), these values are typical for grounded running, while aerial phases, such as in running, do not occur until 1.7 body weight. Finally, the asymmetric curve progression of the total vertical GRF (Fig. 9A) is typical for grounded running, as this also occurs in quails (Andrada et al., 2013a). A further consequence of this context is that grounded running in ants is more likely to occur in steady, fast locomotion than in exploratory behaviour.

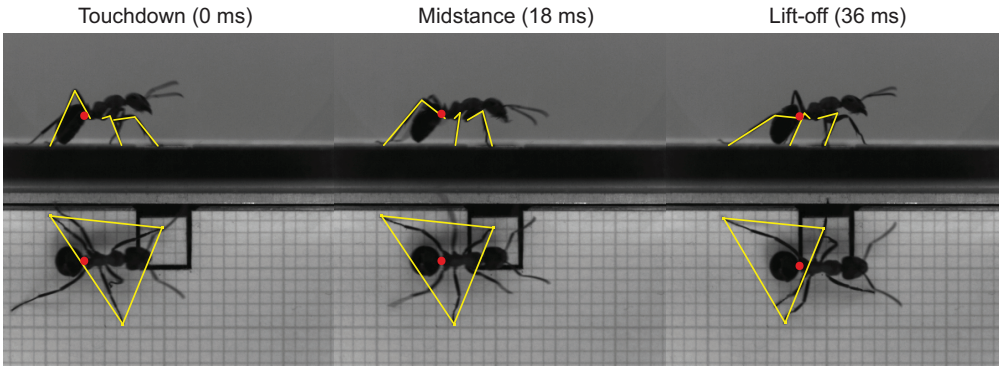

Fig. 10. Exemplary sequence of the contact phase during level locomotion. Running speed: 12.1 cm s^{-1}. The selected frames show the posture of *F. polyctena* at the time of touchdown, midstance and lift-off from the side and from above. In each image a red dot indicates the calculated CoM position. Yellow lines in the sagittal view show the position of the two functional leg segments (femur, tibia–metatarsus–tarsus) with ground contact. Triangles in the top view indicate the support polygon.

The Journal of Experimental Biology (2014) doi:10.1242/jeb.098426

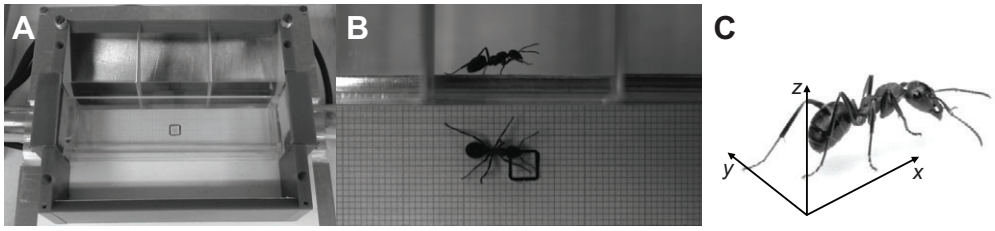

Fig. 11. Experimental setup and coordinate system. (A) Experimental setup from above. The floor was covered with graph paper and the tread of the miniature force plate was embedded in the middle. One sidewall of the track was equipped with optical prisms for an additional side perspective. At both ends, plastic tubes were mounted through which the ants entered and left the experimental runway. (B) Single frame of a video sequence of the locomotion of *F. polyctena*. The kinematics were recorded at 500 Hz with a resolution of 768×512 pixels (0.074 mm pixel^{-1}). (C) The coordinate system.

Conclusions

In conclusion, there is evidence that the investigated ants performed grounded running. This type of gait in small insects combines high running speeds with small vertical oscillations of the CoM necessary to ensure ground contact (Blickhan and Full, 1993). Flight phases would drastically increase the risk of falling, as their habitat is typically strongly structured and extremely rough for ants. Furthermore, the ability to perform fast turns is hereby guaranteed – something that in the wild may be more relevant than energy saving or speed (Gatesy and Biewener, 1991; Daley and Usherwood, 2010). In other words, the fact that a bouncing gait could be identified may be less a matter of efficiency than of control. Even in such a small animal the inertia of the system contributes to the gait pattern, influences its dynamics and may help to improve stability (Ting et al., 1994; Full et al., 2002; Blickhan et al., 2007).

MATERIALS AND METHODS

Animals

The presented studies were conducted between summer and autumn on workers of the local ant species *F. polyctena*. All animals were taken from the same nest in a forest near Jena and subsequently kept in a formicarium in the lab under constant and natural conditions (see Reinhardt et al., 2009). We used nest material as a substrate, wetted at regular intervals, and the ants were fed honey and insects. Part of the formicarium was illuminated by a 60 W daylight lamp in a 12 h rhythm. For an individual experiment, a single ant was randomly removed from the formicarium and weighed by a precision balance (ABS 80-4, Kern & Sohn, Germany). The ants were put into a plastic tube (diameter 12 mm, length 150 mm), which was repeatedly placed via an adaptor at the start and thereafter at the end of an experimental runway (W:H:D: 25×30×90 mm; Fig. 11A). In this way the ants regularly continued steady fast locomotion for 5–20 'rounds' corresponding to total distances of 1.2–4.8 m. This procedure strongly reduced exploratory behaviour and about 10 runs per hour of successful attempts could be completed. Only runs in which the whole runway was crossed straight at constant speed and in which the tread of the force plate was entered with a single leg were selected.

Experimental setup

The kinematics were recorded with an extremely light-sensitive high-speed camera (Fastcam SA3, Photron, San Diego, CA, USA), which reduces the need for additional lighting (LED illumination with a total power of 4 W). One sidewall of the track was equipped with optical prisms so that the motion sequences could be recorded from the sagittal and the horizontal plane synchronously with a single camera (Fig. 11A). The substrate was covered with graph paper and the tread (4×4 mm) of a highly sensitive, three-dimensional, ultra-miniature force plate was embedded in the middle of the runway (Fig. 11B). We used a 3D CAD and simulation software to design the force plate and to calculate its properties by the finite element method. For production of the prototype, we used the stereolithography technology and applied semiconductor strain gages to it (Reinhardt and Blickhan, 2014). Forces as great as 10 µN can be resolved with this sensor and the natural frequencies are above 200 Hz for all directions (see Table 5). A digital amplifier system (MGCplus, Hottinger Baldwin Messtechnik, Darmstadt, Germany) was used to detect the signals of the strain gauges with a sampling rate of 1200 Hz. All further calculations were made in MATLAB R2010a (The MathWorks, Natick, MA, USA). We selected a zero order Savitzky–Golay smoothing algorithm with a box width of 5 points (4.2 ms). Thus, we were able to measure events until 240 Hz without any loss in signal.

Coordinate system

The same system of coordinates was used for the kinematic and dynamic investigations (Fig. 11C). The *x*-axis is parallel to the animal's long axis in the walking direction. The *y*-axis is laterally to the left, parallel to the substrate, and the *z*-axis is perpendicular to the *xy*-plane. Positive GRFs in the forward direction ($\mathbf{F}_x$) accelerate the animal. Positive lateral forces ($\mathbf{F}_y$) accelerate the animal to the left, and positive vertical forces ($\mathbf{F}_z$) push the animal upwards. We do not distinguish between left and right legs. All results on the right side are mapped to the left. Correspondingly, a positive forward directed reaction force observed for the front leg implies pulling and negative force implies pushing. For the left middle leg a positive lateral force implies pulling inwards, and for the hindleg a positive forward component implies pushing outwards.

Kinematic and dynamic analysis

Our entire data set for the dynamic and kinematic analysis included 61 individual runs from 31 different ants. The studied ants had a mean body mass of 21.0±3.7 mg and moved with velocities from 7.8 to 20.8 cm s^{-1}. From this data set we analysed 59 single leg GRF measurements (speed 13.5±3.6 cm s^{-1}, mass 20.9±3.9 mg) consisting of 21 steps of the front leg, 21 steps of the middle leg and 17 steps of the hindleg pair. As confirmed by

Table 5. Specification of the force plate based on FEM simulations and measurements

	x-direction	*y*-direction	*z*-direction
Calculated (FEM) natural frequency (Hz)	379.16	278.93	200.77
Calculated (FEM) spring constant (N mm)	0.1005	0.0691	0.3598
Sensitivity (V N^{-1})	97.84	197.62	51.05
Unfiltered residual noise (±s.d., mV)	1.18±0.33	1.34±0.45	1.39±0.31
Resolvable force after filtering (µN)	5.42	2.87	10.75

FEM, finite element method.

The Journal of Experimental Biology (2014) doi:10.1242/jeb.098426

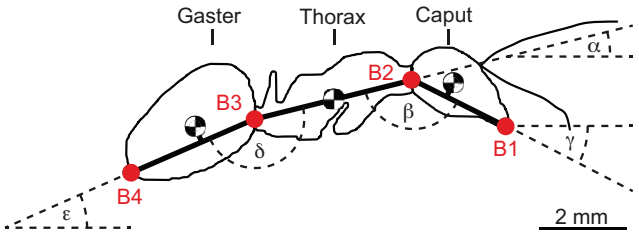

Fig. 12. Body segments and marker positions. Schematic representation of the digitised body markers (B1–B4, red), the estimated positions of the individual segment centres of gravity (represented by the black and white circles) and the calculated angles in the sagittal plane.

our investigations (see Results, 'Three-dimensional body kinematics'), the CoM was located near the petiolus. Therefore, the joint between the petiolus and gaster (Fig. 12, B3) was digitised three-dimensionally in 85 gait cycles of 60 runs (speed 12.5±3.2 cm s^{-1}, mass 21.0±3.7 mg). The complex 3D body kinematics and the stride pattern were studied in 20 gait cycles of 10 runs (speed 11.0±0.7 cm s^{-1}, mass 21.2±2.0 mg). Pseudo-replication was avoided, as we obtained similar results when mean values for individual trials (N=61) instead of individual measurements (N=85) were analysed with the same method (data not shown).

Gait cycle

One finding was that the animals touched the ground first with the middle leg of one tripod (see Results, 'Stride pattern'). A step cycle has therefore been normalised to the contact and the following swing phase of the middle leg. The contact phase starts with the touchdown of the tarsus and ends with the active lifting of the leg. In the hindlegs the tarsus is regularly dragged over the substrate without a significant rise. For this reason, the start of the swing phase was here defined by the moment when the tarsus was moved away from the contact point. For the other two pairs of legs, the swing phase started with the release of the tarsus from the ground. All information in the description of the CoM kinematics is related to the tripod L1/R2/L3 (left front leg, right middle leg and left hindleg).

Digitisation

In order to describe the spatial position of the body segments, the following points (Fig. 12, B1–B4) were digitised three-dimensionally with the software WINanalyze 3D (Version 2.1.1, Mikromak, Berlin, Germany): (i) the distal mandible tip (B1), (ii) the cervix (B2), (iii) the joint between the petiolus and gaster (B3) and (iv) the posterior end of the gaster (B4). The field of vision was about 60 mm wide. Camera resolution was 768×512 pixels, so minimum tracking accuracy was below 0.1 mm. An accuracy of at least 0.05 mm can be assumed as WINanalyze, is able to compute sub-pixel resolutions via interpolating algorithms (Frischholz and Spinnler, 1993). We used the graph paper on the tread to calibrate the video sequences.

Body model and CoM determination

Because of the low leg masses (the sum of all legs is ~10% of the body mass; see Results, 'Mass distribution'), it was assumed that their position has only a small impact on the CoM position. The same applies for the mandibles, antennae and other small appendages (McMeeking et al., 2012). Hence, they were not included in the calculations. The remaining body segments of the ant were separated into three major parts, whereby the gaster (abdomen) and caput (head) each represented one segment. The third segment that we designated as thorax (alitrunk) consists of the remaining parts (mesosoma, petiolus and coxae). This simplification was justified through kinematic preliminary investigations, which indicated that their position relative to each other did not change.

In order to calculate the location of the total CoM, we needed the relative mass and the position of the centre of gravity of each body segment. As we have demonstrated, the mass of each segment correlates with the total mass of the ant and can therefore be calculated as a percentage of the body mass (see Results, 'Mass distribution'). Under the assumption of a homogeneous density distribution, the centroid of a volume is equivalent to the centre of gravity in each segment (McMeeking et al., 2012) (see Fig. 12). Thus, we took a single frame of a typical video sequence to estimate the position of these points and to formulate a geometric relationship concerning the marker points (B1–B4). Accordingly, we determined the gaster centre at a normal distance of 0.35 mm at 4/9 of the distance between B4 and B3. The caput centre was calculated at a normal distance of 0.35 mm at 1/3 of the distance between B2 and B1. The thorax had its centre of gravity in the middle between B2 and B3. Finally, the total CoM position was calculated via the weighted sum of the coordinates of the three segment centres.

Body angles

For describing the sagittal plane kinematics, we calculated five angles (Fig. 12). These were the angles between the thorax and substrate (α), thorax and caput (β), caput and substrate (γ), thorax and gaster (δ), and gaster and substrate (ε). In addition, the angle between the thorax and the x-axis (ζ) was calculated in the transverse plane.

CoM mechanics

To classify the gait into existing models of locomotion, it is imperative to calculate the fluctuations of gravitational potential energy (E_{pot}) and kinetic energy (E_{kin}) of the CoM. As the marker B3 is in very good agreement with the position of the CoM (see Results, 'Three-dimensional body kinematics'), we used its kinematics to calculate the CoM mechanics during the gait cycle. E_{pot} was calculated using the formula: $E_{pot}=\boldsymbol{mgz}$, where m is the mass of the ant, $\boldsymbol{g}$ is the acceleration due to gravity and z is the vertical position of the CoM. For each direction, E_{pot} was calculated via: $E_{pot}=0.5\ m\ v^2$. Whereby v is the velocity in the respective direction, which was determined by temporal derivation of the coordinates. The sum of these energies corresponded to the total energy (E_{tot}) of the CoM. We relied on the phase relationship of E_{pot} and E_{pot} to distinguish running from walking (Ahn et al., 2004). A phase shift of 180 deg between the two energies indicates a walking gait and a shift of 0 deg indicates a running gait (Cavagna et al., 1977). The phase shift is also reflected in the percentage recovery and percentage congruity (Cavagna et al., 1976; Ahn et al., 2004). Ideally, percentage recovery is 100% in a walking trial and 0% in a running trial, while the opposite is true for the percentage congruity. We calculated both values for our data and set a border at 50% congruity to categorise our trials as walking or (grounded) running, following Ahn et al. (Ahn et al., 2004).

Mass distribution

To determine the sub-segment masses, 10 animals were selected that were similar in size and mass to the animals in the dynamic and kinematic studies. The measurements were performed with an electronic precision balance (ABS 80-4, Kern & Sohn) with an accuracy of 0.1 mg. The animals were weighed *in vivo*, then killed by freezing (−18°C). A few hours later, they were individually taken from the freezer and sliced into segments. Thus, we ensured that no mass loss was caused by escaping fluids. The legs were removed distally of the coxae and weighed together.

Acknowledgements

We thank Tom Weihmann and Emanuel Andrada for helpful discussions that led to an earlier version of this manuscript. We also thank two anonymous referees who provided helpful comments on previous drafts of the manuscript.

Competing interests

The authors declare no competing financial interests.

Author contributions

L.R. made significant and substantial contributions to the conception, design, execution and interpretation of the findings being published, and drafting and revising the article. R.B. made significant and substantial contributions to the design, execution and interpretation of the findings being published.

Funding

This work was funded by the German Research Foundation (DFG) [BL 236/20-1 to R.B.].

References

Ahn, A. N., Furrow, E. and Biewener, A. A. (2004). Walking and running in the red-legged running frog, Kassina maculata. *J. Exp. Biol.* **207**, 399-410.

Alexander, R. M. (1966). Rubber-like properties of the inner hinge-ligament of Pectinidae. *J. Exp. Biol.* **44**, 119-130.
Alexander, R. M. and Jayes, A. S. (1978). Vertical movements in walking and running. *J. Zool.* **185**, 27-40.
Andersen, S. O. (1963). Characterization of a new type of cross-linkage in resilin, a rubber-like protein. *Biochim. Biophys. Acta* **69**, 249-262.
Andersen, S. O. (1964). The cross-links in resilin identified as dityrosine and trityrosine. *Biochim. Biophys. Acta* **93**, 213-215.
Andersen, S. O. and Weis-Fogh, T. (1964). Resilin. A rubberlike protein in arthropod cuticle. In *Advances in Insect Physiology*, Vol. 2 (ed. J. W. L. Beament, J. E. Treherne and V. B. Wigglesworth), pp. 1-65. Academic Press.
Anderson, S. O. (1966). Covalent cross-links in a structural protein, resilin. *Acta Physiol. Scand. Suppl.* **263**, 1-81.
Andrada, E., Rode, C. and Blickhan, R. (2013a). Grounded running in quails: simulations indicate benefits of observed fixed aperture angle between legs before touch-down. *J. Theor. Biol.* **335**, 97-107.
Andrada, E., Nyakatura, J. A., Bergmann, F. and Blickhan, R. (2013b). Adjustments of global and local hindlimb properties during terrestrial locomotion of the common quail (*Coturnix coturnix*). *J. Exp. Biol.* **216**, 3906-3916.
Bennet-Clark, H. (2007). The first description of resilin. *J. Exp. Biol.* **210**, 3879-3881.
Biewener, A. A. (1990). Biomechanics of mammalian terrestrial locomotion. *Science* **250**, 1097-1103.
Biknevicius, A. R., Reilly, S. M., McElroy, E. J. and Bennett, M. B. (2013). Symmetrical gaits and center of mass mechanics in small-bodied, primitive mammals. *Zoology* **116**, 67-74.
Blickhan, R. and Full, R. J. (1987). Locomotion energetics of the Ghost crab: II. mechanics of the centre of mass during walking and running. *J. Exp. Biol.* **130**, 155-174.
Blickhan, R. and Full, R. J. (1993). Similarity in multilegged locomotion: bouncing like a monopode. *J. Comp. Physiol. A* **173**, 509-517.
Blickhan, R., Seyfarth, A., Geyer, H., Grimmer, S., Wagner, H. and Günther, M. (2007). Intelligence by mechanics. *Philos. Trans. R. Soc. A* **365**, 199-220.
Cavagna, G. A., Saibene, F. P. and Margaria, R. (1964). Mechanical work in running. *J. Appl. Physiol.* **19**, 249-256.
Cavagna, G. A., Thys, H. and Zamboni, A. (1976). The sources of external work in level walking and running. *J. Physiol.* **262**, 639-657.
Cavagna, G. A., Heglund, N. C. and Taylor, C. R. (1977). Mechanical work in terrestrial locomotion: two basic mechanisms for minimizing energy expenditure. *Am. J. Physiol.* **233**, R243-R261.
Daley, M. A. and Usherwood, J. R. (2010). Two explanations for the compliant running paradox: reduced work of bouncing viscera and increased stability in uneven terrain. *Biol. Lett.* **6**, 418-421.
Delcomyn, F. (1971). The locomotion of the cockroach *Periplaneta americana*. *J. Exp. Biol.* **54**, 443-452.
Duch, C. and Pflüger, H. J. (1995). Motor patterns for horizontal and upside down walking and vertical climbing in the locust. *J. Exp. Biol.* **198**, 1963-1976.
Dudek, D. M. and Full, R. J. (2006). Passive mechanical properties of legs from running insects. *J. Exp. Biol.* **209**, 1502-1515.
Dudek, D. M. and Full, R. J. (2007). An isolated insect leg's passive recovery from dorso-ventral perturbations. *J. Exp. Biol.* **210**, 3209-3217.
Federle, W., Rohrseitz, K. and Hölldobler, B. (2000). Attachment forces of ants measured with a centrifuge: better 'wax-runners' have a poorer attachment to a smooth surface. *J. Exp. Biol.* **203**, 505-512.
Frischholz, R. W. and Spinnler, K. P. (1993). Class of algorithms for real-time subpixel registration. *Proc. SPIE* **1989**, 50-59.
Full, R. (1991). The concepts of efficiency and economy in land locomotion. In *Efficiency and Economy in Animal Physiology* (ed. R. W. Blake), 97-131. Cambridge: Cambridge University Press.
Full, R. J. and Koehl, M. A. R. (1993). Drag and lift on running insects. *J. Exp. Biol.* **176**, 89-101.
Full, R. J. and Tu, M. S. (1990). Mechanics of six-legged runners. *J. Exp. Biol.* **148**, 129-146.
Full, R. J. and Tu, M. S. (1991). Mechanics of a rapid running insect: two-, four- and six-legged locomotion. *J. Exp. Biol.* **156**, 215-231.
Full, R. J., Blickhan, R. and Ting, L. H. (1991). Leg design in hexapedal runners. *J. Exp. Biol.* **158**, 369-390.
Full, R. J., Kubow, T., Schmitt, J., Holmes, P. and Koditschek, D. (2002). Quantifying dynamic stability and maneuverability in legged locomotion. *Integr. Comp. Biol.* **42**, 149-157.
Garcia, M., Kuo, A., Peattie, A. M., Wang, P. C. and Full, R. J. (2000). Damping and size: Insights and biological inspiration. In *International Symposium on Adaptive Motion of Animals and Machines*. Montreal: McGill University.
Gatesy, S. M. (1999). Guineafowl hind limb function. I: Cineradiographic analysis and speed effects. *J. Morphol.* **240**, 115-125.
Gatesy, S. M. and Biewener, A. A. (1991). Bipedal locomotion: effects of speed, size and limb posture in birds and humans. *J. Zool.* **224**, 127-147.
Geyer, H., Seyfarth, A. and Blickhan, R. (2006). Compliant leg behaviour explains basic dynamics of walking and running. *Proc. Biol. Sci.* **273**, 2861-2867.
Gladun, D. and Gorb, S. (2007). Insect walking techniques on thin stems. *Arthropod-Plant Interact.* **1**, 77-91.
Goldman, D. I., Chen, T. S., Dudek, D. M. and Full, R. J. (2006). Dynamics of rapid vertical climbing in cockroaches reveals a template. *J. Exp. Biol.* **209**, 2990-3000.
Graham, D. and Cruse, H. (1981). Coordinated walking of stick insects on a mercury surface. *J. Exp. Biol.* **92**, 229-241.
Heglund, N. C., Fedak, M. A., Taylor, C. R. and Cavagna, G. A. (1982). Energetics and mechanics of terrestrial locomotion. IV. Total mechanical energy changes as a function of speed and body size in birds and mammals. *J. Exp. Biol.* **97**, 57-66.
Hooper, S. L., Guschlbauer, C., Blümel, M., Rosenbaum, P., Gruhn, M., Akay, T. and Büschges, A. (2009). Neural control of unloaded leg posture and of leg swing in stick insect, cockroach, and mouse differs from that in larger animals. *J. Neurosci.* **29**, 4109-4119.
Horstmann, K. (1976). Über die duftspur-orientierung bei waldameisen (*Formica polyctena* Foerster). *Insectes Soc.* **23**, 227-242.
Hughes, G. M. (1952). The co-ordination of insect movements: I the walking movements of insects. *J. Exp. Biol.* **29**, 267-285.
Hutchinson, J. R., Famini, D., Lair, R. and Kram, R. (2003). Biomechanics: are fast-moving elephants really running? *Nature* **422**, 493-494.
Josens, R. B., Farina, W. M. and Roces, F. (1998). Nectar feeding by the ant *Camponotus mus*: intake rate and crop filling as a function of sucrose concentration. *J. Insect Physiol.* **44**, 579-585.
Kimura, T. (1996). Centre of gravity of the body during the ontogeny of chimpanzee bipedal walking. *Folia Primatol. (Basel)* **66**, 126-136.
Kirchner, W. (2001). *Die Ameisen: Biologie und Verhalten*. Munich: Beck C. H.
Koditschek, D. E., Full, R. J. and Buehler, M. (2004). Mechanical aspects of legged locomotion control. *Arthropod Struct. Dev.* **33**, 251-272.
Larsen, G. S., Frazier, S. F., Fish, S. E. and Zill, S. N. (1995). Effects of load inversion in cockroach walking. *J. Comp. Physiol. A* **176**, 229-238.
Lipfert, S. W., Günther, M., Renjewski, D., Grimmer, S. and Seyfarth, A. (2012). A model-experiment comparison of system dynamics for human walking and running. *J. Theor. Biol.* **292**, 11-17.
McMahon, T. A., Valiant, G. and Frederick, E. C. (1987). Groucho running. *J. Appl. Physiol.* **62**, 2326-2337.
McMeeking, R. M., Arzt, E. and Wehner, R. (2012). Cataglyphis desert ants improve their mobility by raising the gaster. *J. Theor. Biol.* **297**, 17-25.
Michels, J. and Gorb, S. N. (2012). Detailed three-dimensional visualization of resilin in the exoskeleton of arthropods using confocal laser scanning microscopy. *J. Microsc.* **245**, 1-16.
Muir, G. D., Gosline, J. M. and Steeves, J. D. (1996). Ontogeny of bipedal locomotion: walking and running in the chick. *J. Physiol.* **493**, 589-601.
Neff, D., Frazier, S. F., Quimby, L., Wang, R. T. and Zill, S. (2000). Identification of resilin in the leg of cockroach, *Periplaneta americana*: confirmation by a simple method using pH dependence of UV fluorescence. *Arthropod Struct. Dev.* **29**, 75-83.
Nyakatura, J. A., Andrada, E., Grimm, N., Weise, H. and Fischer, M. S. (2012). Kinematics and center of mass mechanics during terrestrial locomotion in northern lapwings (*Vanellus vanellus*, Charadriiformes). *J. Exp. Zool. A* **317**, 580-594.
Patek, S. N., Dudek, D. M. and Rosario, M. V. (2011). From bouncy legs to poisoned arrows: elastic movements in invertebrates. *J. Exp. Biol.* **214**, 1973-1980.
Pelletier, Y. and Caissie, R. (2001). Behavioural and physical reactions of the Colorado potato beetle, *Leptinotarsa decemlineata* (Say) (Coleoptera: Chrysomelidae) walking on a slanted surface. *Biol. Cybern.* **84**, 269-277.
Reilly, S. M., McElroy, E. J. and Biknevicius, A. R. (2007). Posture, gait and the ecological relevance of locomotor costs and energy-saving mechanisms in tetrapods. *Zoology* **110**, 271-289.
Reinhardt, L. and Blickhan, R. (2014). Ultra-miniature force plate for measuring triaxial forces in the micronewton range. *J. Exp. Biol.* **217**, 704-710.
Reinhardt, L., Weihmann, T. and Blickhan, R. (2009). Dynamics and kinematics of ant locomotion: do wood ants climb on level surfaces? *J. Exp. Biol.* **212**, 2426-2435.
Rubenson, J., Heliams, D. B., Lloyd, D. G. and Fournier, P. A. (2004). Gait selection in the ostrich: mechanical and metabolic characteristics of walking and running with and without an aerial phase. *Proc. Biol. Sci.* **271**, 1091-1099.
Ruina, A., Bertram, J. E. A. and Srinivasan, M. (2005). A collisional model of the energetic cost of support work qualitatively explains leg sequencing in walking and galloping, pseudo-elastic leg behavior in running and the walk-to-run transition. *J. Theor. Biol.* **237**, 170-192.
Sannasi, A. (1969). Resilin in the cuticle of click beetles. *J. Georgia Entomol. Soc.* **4**, 31-32.
Schmitt, D. (1999). Compliant walking in primates. *J. Zool.* **248**, 149-160.
Schmitt, D. (2003). Insights into the evolution of human bipedalism from experimental studies of humans and other primates. *J. Exp. Biol.* **206**, 1437-1448.
Schmitt, J., Garcia, M., Razo, R. C., Holmes, P. and Full, R. J. (2002). Dynamics and stability of legged locomotion in the horizontal plane: a test case using insects. *Biol. Cybern.* **86**, 343-353.
Seidl, T. and Wehner, R. (2008). Walking on inclines: how do desert ants monitor slope and step length. *Front. Zool.* **5**, 8.
Sponberg, S. and Full, R. J. (2008). Neuromechanical response of musculo-skeletal structures in cockroaches during rapid running on rough terrain. *J. Exp. Biol.* **211**, 433-446.
Srinivasan, M. and Holmes, P. (2008). How well can spring-mass-like telescoping leg models fit multi-pedal sagittal-plane locomotion data? *J. Theor. Biol.* **255**, 1-7.
Srinivasan, M. and Ruina, A. (2006). Computer optimization of a minimal biped model discovers walking and running. *Nature* **439**, 72-75.
Ting, L. H., Blickhan, R. and Full, R. J. (1994). Dynamic and static stability in hexapedal runners. *J. Exp. Biol.* **197**, 251-269.
Weihmann, T. and Blickhan, R. (2009). Comparing inclined locomotion in a ground-living and a climbing ant species: sagittal plane kinematics. *J. Comp. Physiol. A* **195**, 1011-1020.
Weis-Fogh, T. (1960). A rubber-like protein in insect cuticle. *J. Exp. Biol.* **37**, 889-907.
Zollikofer, C. (1994). Stepping patterns in ants – influence of speed and curvature. *J. Exp. Biol.* **192**, 95-106.